

# WET FIBRE SURFACE – DOES IT BEHAVE LIKE A GEL?

*Annika E. Ketola<sup>1,\*</sup>, Miika Leppänen<sup>2</sup>, Tuomas Turpeinen<sup>1</sup>, Petri Papponen<sup>2</sup>, Anna Sundberg<sup>3</sup>, Kai Arstila<sup>2</sup> and Elias Retulainen<sup>1</sup>*

<sup>1</sup> VTT Technical Research Centre of Finland Ltd, P.O. Box 1603, FI-40101 Jyväskylä, Finland

<sup>2</sup> University of Jyväskylä, Nanoscience Center, Department of Biological and Environmental Science, FI-40014 Jyväskylä, Finland

<sup>3</sup> Åbo Akademi University, Johan Gadolin Process Chemistry Center, Porthansgatan 3, FI-20500 Åbo/Turku, Finland

## ABSTRACT

The physico-chemical characteristics of wet fibre surfaces and their role in fibre bonding and paper properties have been under debate and research for decades. The gel-likeness of the fibre surfaces has been addressed in many studies but has not been explicitly demonstrated. In this study, the structure of wet beaten kraft pulp fibre surface and its similarity with microfibrillated cellulose (CMF) was shown using helium ion microscopy (HIM) imaging. Beaten kraft fibres and CMF were dried using two mild drying methods to preserve the delicate fibrillated structures. The fibre surface had a strong resemblance with gel-like CMF material. The amount of external fibrillation varied along the fibre length and was often shown to extend tens of micrometers from the fibre surface. The gel-like behaviour of wet fibrillated material was demonstrated using rheological tests. The examined CMF and CNF samples with solids contents of 1.97% and 1.06%, respectively, showed gel-like behaviour. A low gelling point suggests that fibrillated fibre surfaces have the ability to transfer forces at very

\* Corresponding Author: annika.ketola@vtt.fi

low consistencies, and that the ability increases as a power function of the solids content. This is assumed to play a remarkable role in increasing inter-fibre adhesion and in transmitting inter-fibre forces within consolidating webs, whether arising from external tensions or internal drying stresses.

## INTRODUCTION

The properties and appearance of wet fibre surfaces and their effect on fibre bonding have been under extensive research for decades. Strachan [1] and Clark [2], [3] were among the firsts ones to state that in a wet state, the external fibrils on the fibre surface are important components contributing to inter-fibre bonding. Nanko and Ohsawa [4] showed using transmission electron microscopy (TEM) that the interphase between bonded fibres in papers composed of an amorphous-appearing layer consisting of the external microfibrils and secondary fines contributing to the strength of the interfibre bond. This layer was designated a “bonding layer” and was said to have a film-like structure. Pelton et al. [5] hypothesised that in a wet state, fibre surfaces consist of a gel-like layer of hydrated fibrils and hemicelluloses.

Refining has been the main method applied for improving the strength of paper made of chemical pulps and external fibrillation has been named as one of the primary effects of refining [6], [7]. External and internal fibrillation together with the creation of fines have definite increasing effect on fibre bonding, wet web-, and dry strength of paper [8]. The quantification of the separate role of external fibrillation is difficult. However, separate addition of fibril material, such as fines, microfibrillated cellulose (CMF) [9]–[12] and nanocellulose (CNF) [13], is known to strongly increase paper strength. For example, as much as a 15% addition of fines to kraft or CTMP fibres have been shown to increase tensile strength significantly (136%–1670%) [14], [15] and CMF has been shown to have a similar effect [16], [17]. The effect of fines depends highly on the used fibre material. With stiff mechanical fibres, the effect is stronger when compared to more flexible chemical pulp fibres. The external fibrillation can be expected to have a similar role.

Fibrillated cellulose materials are extracted from plant cell walls using only mechanical fluidisation [9], [18] or its combination with chemical [13] or enzymatic treatments [19]. Depending on the preparation method and raw material used, the fibril dimensions and morphology can vary a lot [20]. The fibril widths are between 1–100 nm while length is on a micrometer scale. Thus, the aspect ratio and specific surface areas of fibrillated celluloses are very high. Aspect ratios varying between 100–370 [21], [22] and specific surface areas from 30 to

100 m<sup>2</sup>/g for CMF [23], [24] and even 400–500 m<sup>2</sup>/g for CNF [25], [26] have been reported. Due to this, fibrillated materials have been shown to possess a gel-like character at low solid contents (0.1–0.4%) in rheological tests [19], [27]. In terms of rheology, gel is a viscoelastic material which possesses both viscous and elastic behaviour under stress. A dispersion can be assumed to be a gel when the elastic properties dominate the viscoelastic behaviour, meaning that the storage modulus ( $G'$ ) is larger than the loss modulus ( $G''$ ) and the phase angle ( $\delta$ ) is  $45^\circ > \delta > 0^\circ$  [28].

As fibrillated cellulose originate from the fibre wall, it is natural that they are considered to be a representative model for cellulose fibre surfaces having similar physical and mechanical properties. This approach has been utilised especially in adsorption and interaction studies using quartz crystal microbalance (QCM) and atomic force microscopy (AFM) [29]–[33]. The similarities between fibrillated materials and fibre surface, including the actual gel-likeness and the corresponding rheological characteristics, are challenging to prove explicitly. However, there is implicit evidence on the matter utilising high resolution imaging and surface analytical methods. Myllytie et al. [34] studied wet CMF and cellulose fibre surfaces using optical and scanning electron microscopy (SEM) and QCM. The dispersing and aggregating effects of polymer additives on the CMF and fibre surfaces were similar and the gel-likeness of the fibre surfaces was used to explain the polymer adsorption behaviour. Chhabra et al. [35] also showed with AFM that there is a compliant fibrillar layer on the fibre surface and that the fibre beating increases the thickness of this layer. The thickness of this layer was estimated to be hundreds of nanometers. Water retention value (WRV) is a simple method to analyse external and internal fibrillation of fibres and it has also been applied to fibrillated cellulose materials [36]. Fibrillated cellulose materials have WRV values from 6 g/g to 16 g/g depending on the degree of fibrillation. In general, the WRV of cellulose fibres is around 1 g/g (centrifuged at 3000 g for 15 minutes) and fibre refining increases the WRV of fibres as the fibre surface fibrillation and specific surface area increases binding more water (and possibly turning more gel-like).

SEM is an excellent tool to study material surface morphology and characteristics. It has been used for imaging the ultrastructure of fibre surfaces [37]–[39] and fibrillated cellulose [40]–[42]. Recently, a new powerful imaging technique, scanning helium ion microscopy (HIM), has entered the imaging field [43]. HIM has drawn attention due to its better resolution, higher depth of field than SEM and the possibility to image non-conductive samples without coating. This is because the charging caused by helium ions can be compensated for with an electron flood gun [44]–[46]. High surface contrast can be achieved without the need for sample coating and HIM was also a more delicate method for biological samples. In addition to fibres, HIM has also been used in the detection of other

cellulose-based materials like CNF [25], [47], [48], cellulose nanocrystals [44], [48] and CNF-kaolin composites [49]. However, no direct comparison of fibre surface fibrils and fibrillated cellulose materials have been done using the powerful imaging methods.

The objective of this study was to characterise the surface of wet kraft pulp fibres using HIM imaging. The hypothesis was that the surface of beaten kraft pulp fibres is composed of microfibrillated cellulose and that this material behaves like a gel. Both fibres and CMF samples were imaged with HIM without sample coating to analyse the similarity between the wet CMF and fibre surfaces. In order to maintain the wet fibrillated structures in as natural a state as possible, they were dried using two mild drying techniques, i.e., critical point drying (CPD) and freeze drying preceded by cryofixing in liquid propane. These methods have previously been used in the preparation of CNF aerogels and they have been shown to preserve the delicate fibrillated structures well [23], [25], [50]. In our previous study [25], CPD exhibited a higher specific surface area for nanofibrillated cellulose (SSA 386 m<sup>2</sup>/g) than freeze drying from liquid-propane (SSA 172 m<sup>2</sup>/g) and is a recommended technique if very delicate structures are studied. However, CPD is more laborious and time-consuming than freeze drying and involves the use of solvents. Here, both methods were applied to estimate whether any significant differences are observed when drying microfibrillated cellulose and fibres. In addition, the effect of carboxymethyl cellulose (CMC) on fibre surface fibrillation was also studied as it has been said to increase the gel-likeness of the fibre surfaces [31], [51].

Rheological measurements of microfibrillated cellulose at low solids content was carried out to determine the viscoelastic properties and gel-like behaviour of CNF and CMF. Two criteria were used for evaluating the gel-likeness of the materials: (1) Material can be assumed to behave like a gel if the phase angle is <45°, and (2) the storage modulus  $G'$  is much higher than the loss modulus  $G''$ . In the experiment, the storage modulus ( $G'$ ) and loss modulus ( $G''$ ) of the material were determined and the ratio between  $G'$  and  $G''$  was used to characterise the material properties.

## **MATERIALS AND METHODS**

### **Chemicals**

Liquid propane (class 2, UN 1965: 95% propane and 5% butane) was purchased from AGA. Liquid nitrogen (ABB) was received from the University of Jyväskylä. Acetone (≥99.9%) was purchased from Sigma. Ethanol (absolute AA, Etax) was obtained from Altia Industrial. Sodium carboxymethyl cellulose, CMC,

(MW 700 kDa, DS 0.800.95, Aldrich) was received in a dry form. CMC was diluted to a 1% solution with deionised water, heated to a boil and kept under agitation until clearly dissolved.

### **TEMPO-oxidised Cellulose Nanofibrils (CNF) and Cellulose Microfibrils (CMF)**

CNF was prepared from never-dried birch kraft pulp by TEMPO-mediated oxidation and fluidisation. TEMPO-mediated oxidation was performed as previously described [13]. Fibres were oxidised using TEMPO-reagent, sodium bromide and NaClO in pH 10 at room temperature. After oxidation, fibres were microfluidised using two passes (Microfluidiser M7115-30).

CMF was prepared from bleached, never-dried birch kraft pulp by mechanical disintegration [52]. The dispersed pulp (1.7% consistency) was first pre-refined with a grinder (Supermasscolloider MKZA10-15J, Masuko Sangyo Co.) at 1,500 rpm, followed by treatment with a fluidiser (Microfluidics M-7115-30). The CMF was produced after five passes at an operating pressure of 1,800 bar. No chemical modification was applied.

### **Kraft Fibres**

The fibres used in the experiments were bleached softwood kraft pulp from a pulp mill in central Finland. The pulp was refined with a Prolab refiner (Valmet, Finland) using conical fillings and using specific refining energy of 135 kWh/t to SR 25 (at 3.6% consistency). Fibre, fines and crill properties were determined using an L&W Fibre Tester Plus analyser (ABB), and the results are shown in Table 1. The fibre measurement system is based on optical image analysis in which single fibres are investigated in a water-fibre suspension. The crill measurement uses ultraviolet (UV) and infrared (IR) light to give a relative number for the macrofibrillated and also for part of the microfibrillated material in the sample, also including the fibrils attached to the fibres. With the UV light, both fibres and crill can be detected, while IR sees only fibres. Results are given as a dampening ratio of UV/IR light. The ratio is a relative number and it does not depend on the fibre concentration. A more detailed description about the crill measurement can be found in related literature [53], [54].

**Table 1.** Kraft pulp (SR25) fibre properties and crill quota

<i>Mean length</i>	<i>Mean width</i>	<i>Mean shape</i>	<i>Mean fines content</i>	<i>Crill Quota (UV/IR)</i>
2.073 mm	30.0 µm	86.9%,	19.0%	1.118

## Mild Drying Methods

Two mild drying methods were applied: (1) Plunge freezing (cryofixing) followed by freeze drying and (2) critical point drying (Figure 1). Kraft pulp was used as a 1.6% fibre slurry and CMF was used as a 1% solution. In cryofixing, a drop of CMF/fibre solution was placed on a TEM grid (300 mesh)/membrane (Millipore, ME25, 0.45  $\mu\text{m}$  pore size) and immediately plunged in liquid-propane (propane gas was liquefied using liquid nitrogen). Cryofixed samples were placed on a cooled metal plate (cooled using liquid nitrogen) and dried in a freeze drier at  $-50\text{ }^{\circ}\text{C}$  at 0.520 mbar (Christ LOC-1m) over night. The dried samples were kept in a desiccator until HIM-imaging.

The critical point drying (CPD) process was started with a solvent exchange with ethanol and acetone by first dehydrating the samples of CMF and kraft fibres in the ethanol (absolute) step series 50%, 70%, 90%, 95%, 99.5% and 99.5%. Each step was 30 minutes. The final step was done in acetone overnight. A critical point dryer (Leica CPD 300) was used to dry the samples from ethanol or acetone. The CPD programme included 16 exchange cycles of  $\text{CO}_2$  at medium speed (speed value 5) without stirring. Slow speed was used for gas fill, heating, and venting steps. For HIM imaging, the dried samples were attached to metal stubs using the carbon tape and kept in a desiccator until HIM imaging.

## Helium Ion Microscope-imaging

A helium ion microscope (Zeiss Orion Nanofab) was used for imaging the mild-dried CMF and fibre samples. An acceleration voltage of 30 kV and an ion current in the range of 0.1 pA were used. A beam aperture was 10  $\mu\text{m}$ , line averaging was 8 or 16 lines, dwell time 1.0  $\mu\text{s}$  and working distance 9 mm. An image size was set to 1024 x 1024 pixels. All samples were studied without coating and an elec-

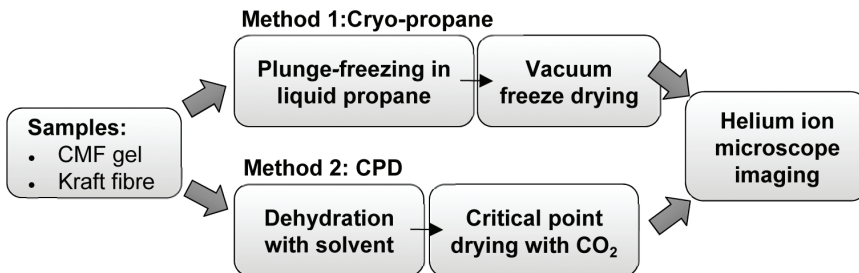


**Figure 1.** Sample preparation chart of wet CMF and kraft fibre samples for imaging with HIM. Two mild drying methods were applied: freeze drying and critical point drying.

tron beam from flood gun (energy 750 eV) was used to neutralise the charges in the sample. Pressure in the measurement chamber was approximately  $1 \cdot 10^{-7}$  Torr.

## **Rheology**

Viscoelastic properties of CNF at 1.06% consistency and CMF at 1.97% consistency were measured using a hybrid rheometer (TA Instruments, Discovery HR-2) with flat plate geometry (20 mm diameter) in oscillation mode. The operating gap was adjusted to 1,500  $\mu\text{m}$ . The temperature was set at 22 °C. A metal cover was used to minimise sample evaporation. Measurements were repeated four times. The oscillation strain sweeps from 0.01 to 10% at the angular frequency of 1 Hz were carried out to define the linear viscoelastic regimes. Then the oscillation frequency sweeps in the range of 0.1–100 rad/s at 0.1% strain for CMF and at 1.0% strain for CNF was performed.

## **RESULTS AND DISCUSSION**

### **Surface Morphology of CMF and Fibrillated Kraft Fibres**

Materials dried with mild drying methods, such as freeze drying and CPD, are often called aerogels [55]. HIM images of fibres and the CMF material dried with the mentioned methods can be seen in Figure 2 and Figure 3. The examined CMF showed similar highly porous structure after mild drying (Figure 2a,b,c). Density, porosity and specific surface area of CMF dried using freeze drying (with cryopropane fixing) has been reported to be 0.02  $\text{g}/\text{cm}^3$ , 98.7% and 70  $\text{m}^2/\text{g}$ , respectively [23]. Due to the high surface area and low density, CMF aerogel is interesting material, for example, for sensor- and oil-absorbent applications [50], [56].

The challenge in preparing wet samples for microscopy is how to retain the original high surface area and avoid the coalescence of fibrils during drying. In our recent study [25], it was shown that although freezing CNF sample in liquid nitrogen and subsequent vacuum drying yields a relatively high surface area (42  $\text{m}^2/\text{g}$ ), the freezing in liquid propane gives even higher surface areas (172  $\text{m}^2/\text{g}$ ), but the highest values were obtained with critical point drying (375  $\text{m}^2/\text{g}$ ). In this work, the difference between freeze drying and CPD was also observed. Freeze dried samples (Figure 2a,d) seemed to have bigger pores in cell-like structure and more film formation. Film formation is an indication of the formation of ice crystals during the drying process, meaning that the sample cryofixing and freeze drying has not been optimal [57], [58]. The appearance of CPD dried samples (Figure 2b,e) was more fluffed, showing no clear film formation and better separation of fibril structure. When using the CPD method, the

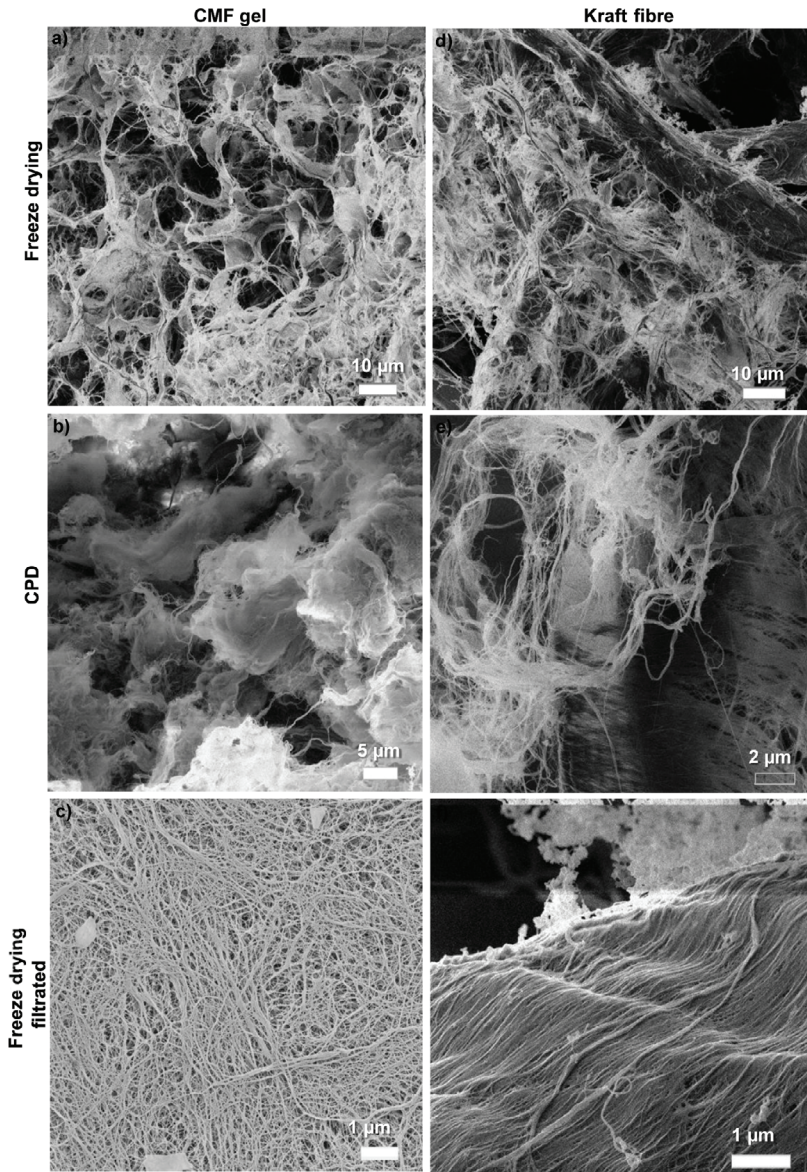


**Figure 2.** HIM images of kraft-fibre surfaces (right row) and CMF samples (left row) dried with different mild drying methods: (a), (b) cryo-propane freeze dried; (c), (d) CPD; and (e), (f) cryo-propane freeze-dried (CMF sample was filtrated to 15% DSC with centrifugation before freezing).



water in the sample is exchanged for ethanol/acetone. The hydrogen bonding between cellulose hydroxyl groups is hindered, which can result in better separation of fibrils in the dried structure [25].

The external fibrillation of fibres (Figure 2d,e and 3) was seen as partly detached and separated surface fibrils from the more solid fibre surface. The fibril material appeared white and was distributed unevenly over the fibres, extending even tens of micrometers from the fiber surface. Primary wall layer P and often also S1 are usually detached from fibre surfaces during pulping and refining, hence revealing the S2 layer [46], [59] so fibrillated material on the fibres may originate from the S1 and S2 layers. In Figure 3, the high fibril angle of the fibre surface suggests that there is still some S1 layer left but in Figure 2f, the S2 layer seems to be fully revealed. The detached surface fibrils on fibres showed high resemblance with CMF, especially between the freeze-dried samples (Figure 2a,d), although fibrils had more parallel orientation.

One of the CMF samples was filtrated to 15% dry solid content with centrifugation before cryofixing in propane (Figure 2c). The appearance of filtrated CMF was more compact than directly-fixed samples but fibrils were still separated showing that already at that low dry solids content the fibrillar structure is consolidated. The filtrated CMF sample had similarities with a fibre S2 layer, where, however, the fibrils are parallel and still more closely attached to the fibre wall. A clear difference between the fibre S2 surface layer (Figure 2f) and CMF (Figure 2c) is the high degree of orientation of fibrils in the S2 layer compared to a more random orientation in the CMF sample. A certain waviness suggests that the fibre surface was swollen.

Both CMF and fibre surfaces began to break down during imaging at high resolutions in a similar way, which has been observed with CNF [25]. This may be due to the ionization of the cellulose by the ion beam, which breaks down the more loosely bound amorphous regions in the cellulose structure.

### **Imaging of Fibre Surfaces with CMC**

Subsequently, the effect of CMC on wet fibre surfaces was examined. Samples of pure CMC solution and CMC in fibre suspension were cryofixed and freeze dried. As with CMF, an aerogel-like structure was also achieved with CMC (Figure 4a,b). However, a pure CMC structure resembled more agar [60] than CMF, due to its denser structure and smaller pore size.

CMC-treated fibres were more fibrillated compared to additive-free ones (Figure 4c,d), being surrounded and covered with very thin fibril strands. Unlike with pure CMC, where both film- and fibril-like structures could be observed, CMC added to fibres showed only fibril-like structures. Myllytie et al. [31] have shown that absorption of CMC onto CMF model fibrils and fibre surface causes

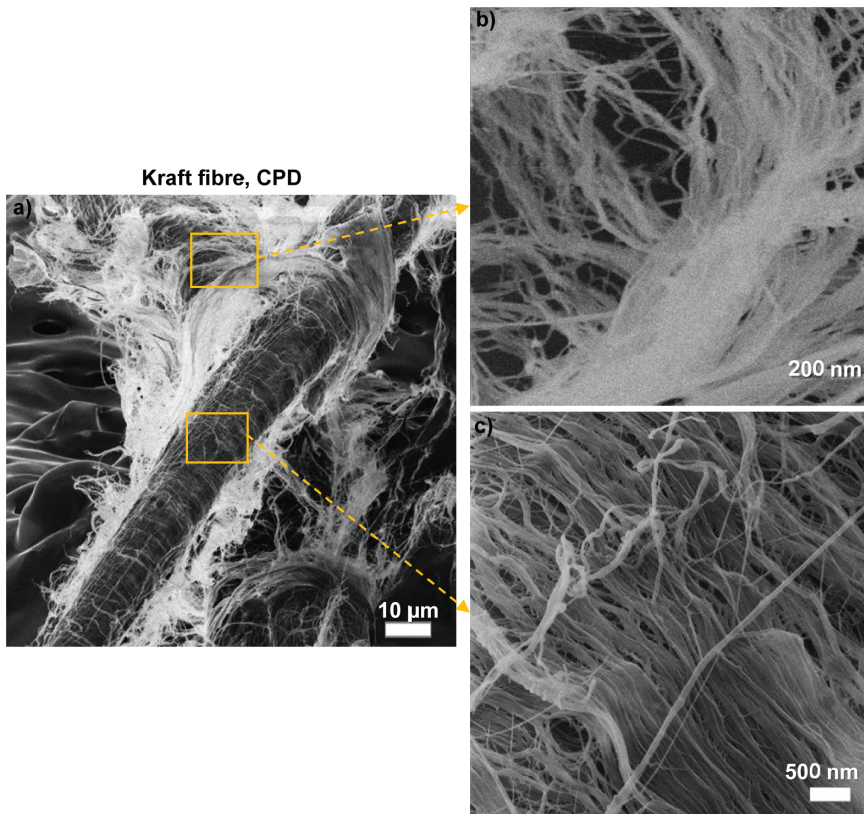


**Figure 3.** HIM images of CPD-dried kraft fibre with different magnifications.

dispersion of fibrils. This is probably the main reason for the high fibrillation of CMC treated fibre samples. However, in addition to that, Figure 4b shows that also CMC forms some fibril-like structures on its own.

As mentioned before, HIM also causes some degradation of the thin fibrils of the samples at high magnification. Interestingly, there was no notable degradation of the pure CMC or CMC-treated fibres even when imaging at high magnifications. This suggests that part of the observed higher number of small fibril strands of CMC-treated fibres may be due to their superior resistance to degradation. Ershov [61] observed that functionalised cellulose-derivates, including CMC, do not degrade as much as pure cellulose during radiation treatment. Thus, HIM could be an interesting technique for nanoscale structural characterisation of derivatised paper additives.

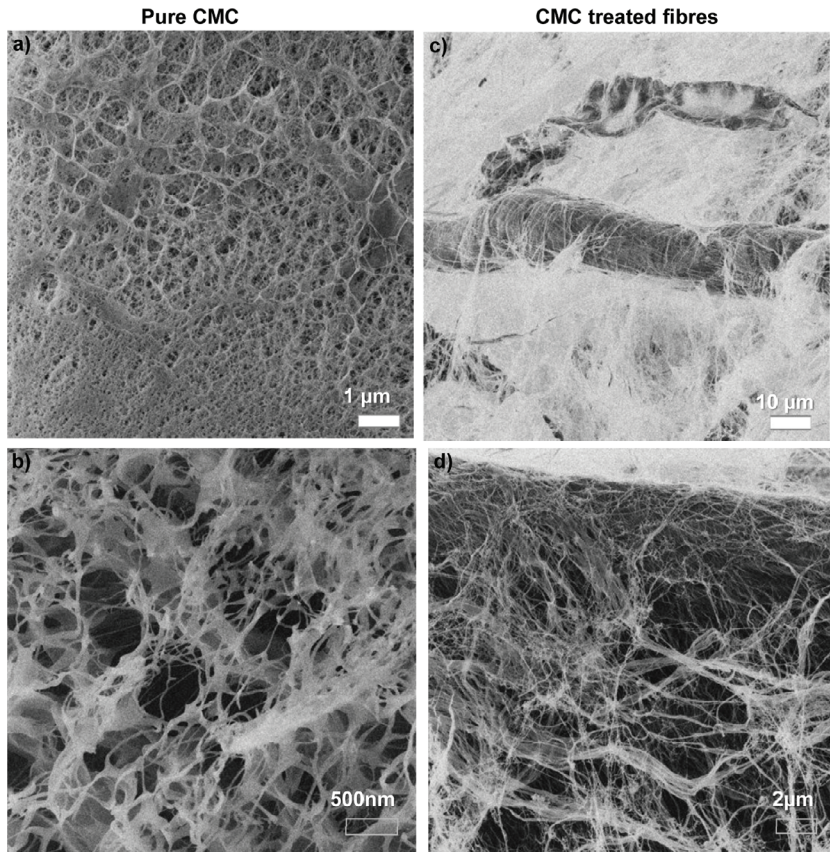


**Figure 4.** HIM images of (a), (b) kraft fibres with CMC and (c), (d) CMC dried with cryopropane with different magnifications.

### Viscoelasticity of Wet CMF and CNF

Wet CMF and CNF materials were used for model materials for fibre surface fibrillation and their viscoelastic and possible gel-like behaviour was tested using a rheometer. CMF and CNF samples were tested at consistencies of 1.97% and 1.06%, respectively. The mean values of oscillation amplitude-, and frequency sweep measurements are shown in Figure 5. Both CMF and CNF had the phase angle below  $45^\circ$  (Figure 5a). The wet CMF sample had higher storage modulus than the CNF samples, which can be explained by the higher dry solid content (DSC) of CMF.  $G'$  and  $G''$  values did not depend on the frequency (Figure 5b).

Arola et al. [27] showed independently that Tempo-oxidised CNF has the critical gel point at 0.4% consistency. Thus, the behaviour of the oxidised CNF at 1.06% consistency was far above the gelling point and the elastic behaviour (described by the storage modulus,  $G'$ ) dominated over the viscoelastic behaviour (described by the loss modulus,  $G''$ ). The same applies to CMF at 1.97% concentration as it has been shown to behave like a gel in the concentration range 0.1% to 6% [19]. The gel-like behaviour of CMF and CNF materials have been addressed in many studies before [19], [62], [63] as well as the strong power law dependence of the storage modulus on the DSC of the cellulosic material. The yield point has been shown to increase proportionally in step with the consistency to the power of 2.3 [64].

The results of this study and earlier studies [19], [27] show that the gelling point of CNF and CMF material is below 1% consistency and above that, the elastic behaviour dominates over the viscoelasticity. With increasing solids content, the storage modulus increases rapidly indicating that the material becomes more and more solid-like and is also able to transmit higher stresses. At 15% dry solids content, the CMF already looked consolidated (Figure 2). Due to the low gelling point of CMF, it can be assumed that a low amount of fibrillated

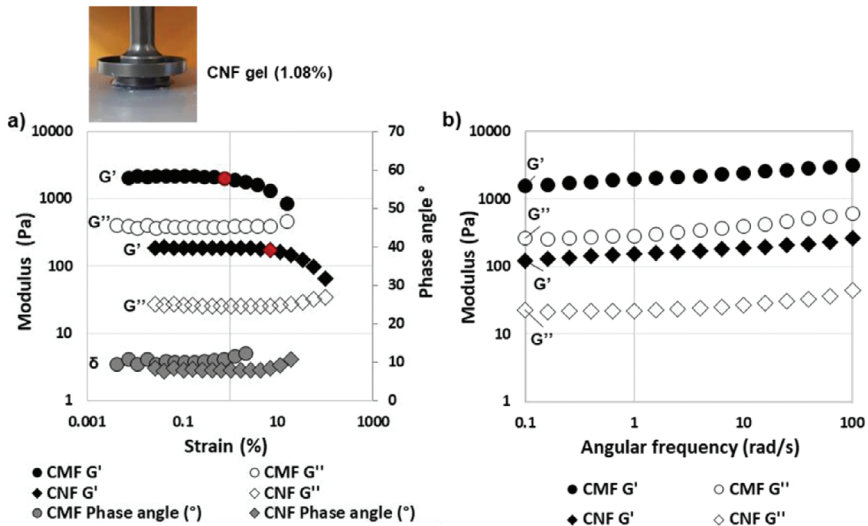


**Figure 5.** (a) Oscillation amplitude-sweep as a function of oscillation strain (%) and (b) Frequency sweep as a function of angular frequency (rad/s) of CMF (sphere) and CNF (square) CNF. Storage modulus ( $G'$ , black), loss modulus ( $G''$ , white) and phase angle ( $\delta$ , grey). Red marks indicate the strain values where the material structure starts to break.

material on fibres creates a gel-like surface, which can have several effects. For example, a gel-like surface has an impact on the fibre rheology, fibre swelling, polymer adsorption on fibres and fibre shrinkage during drying, which again affect the water retention during the formation process and the strength of fibre-fibre bonding in the dry structure [33]–[35].

Gel material has high conformability and it probably has a strong effect on increasing molecular contact area within a fibre-fibre bond [65], [66]. Chhabra et al. showed that the thickness of the soft compliant layer on fibre is hundreds of nanometers [35]. However, the images shown here indicate that the gel-like material can actually extend even tens of micrometers from the fibre surface (Figure 3). The low gelling point and high conformability of fibrillated materials indicate that it can both increase the molecular contact area within a fibre-fibre bond and deliver forces already at low dry solids content. This explains why a small addition of fibrillated material can considerably increase the wet web, and dry strength of paper [67]–[69].

The gel-likeness of the fibre surface was also found to vary along the fibre length. With the studied mildly refined pulp (SR25), some wet fibre surfaces showed a nearly smooth S2 layer surface without notable fibrillation. This type of clean fibre surface can have a lower bonding ability than fibrillated surfaces. This may offer an explanation of why the inter-fibre bonds between two very flat fibres may have a low actual contact area [66]. The exposure of the S2 layer, however, means that the S1 layer has been removed and it probably can be found in the fine fraction of the pulp. Increased refining degree would have resulted in a higher amount of fibrillation and more fibrillation originating from the S2 layer, which could lead to a stronger contribution to interfibre bonding like the fines created at later stages of refinement [15].

The dispersion of fibrils is promoted by a higher charge, which probably also contributes to a reduced gel-point of the fibrillated material. A swollen gel-like fibril layer occupies a rather high volume and is mechanically soft and conformable. With increasing solids, the gel-like layer becomes more dense and less soft [19] and is able to transfer higher forces. Thus, for good bonding, the fibre surfaces need to come into contact at very low solids content in order to fully utilise the bonding potential of the gel-like layers.

The mechanical cohesion of CMF at wet pressing solid contents (~30% DSC) is already high and it can transmit high forces from one fibre to another. It also has an increasing effect on the shrinkage behaviour of the fibre network, as the “the adhesion before shrinkage” forces [70] are at a higher level. For a web that dries under restraint, this results in higher tensile stiffness and elastic modulus due to better fibre segment activation [7], [71], [72]. For a web allowed to shrink freely, this means that the shrinkage of fibres is transmitted to the shrinkage of the web at a higher degree, resulting in a higher elongation potential of the paper.

The high surface area of fibrillated and gel-like surface layers presumably tends to promote adsorption of chemical additives and fillers by offering connection points. The HIM images of CMC-treated fibres suggest that adsorbed CMC increases the dispersion of fibrils, but it is also capable of making fibril-like strands that can connect surfaces. CMC has been shown to form a soft gel on cellulose that enhances the paper properties significantly [51]. The softer and more swollen the layer, the higher the increase in the tensile properties was observed. CMC is known to increase fibril dispersion on fibre surfaces [34], decrease friction between fibres in suspension and increase the wet web and dry strength of paper [73]–[75].

Based on the presented results, it seems clear that wet fibrils, whether on fibrillated fibres or as separate fibril material, seem to behave like a gel and have the potential to affect various mechanical properties of wet and dry fibre networks.

## CONCLUSIONS

The following conclusions were made based on the investigations of fibrillated fibre surfaces and pure CMF material carried out by using mild drying methods, helium ion microscopy and rheometry:

- 1 Two mild drying methods (CPD and freeze drying) were used to dry CMF and fibre samples to estimate whether any significant differences are observed. Both methods provided similar results, but CPD showed better fibril separation and higher specific surface area than freeze drying. However, CPD is a more laborious and time-consuming technique than freeze drying and includes the use of solvents. When selecting a suitable drying method for fibrillated materials, one can consider whether it is necessary to use a laborious method and have highly preserved structure.
- 2 Fibrillation on a wet fibre surface had a striking resemblance to pure CMF material imaged with helium ion microscopy, suggesting that they basically have similar structure and properties. Fibrillated materials are gel-like already at very low solids content (<1%), meaning that only a small amount of fibrils on fibres can result in a gellike behaviour ( $G' > G''$  and  $\delta = 45^\circ > \delta > 0^\circ$ ).
- 3 The amount of external fibrillation was shown to vary along the fibre length and extended even tens of micrometers from the fibre surface. This means that the gel-like behaviour of the fibre surface can also vary correspondingly. An increase in the dry solids content of the fibrillated material (following a power function) leads to a strongly increased elastic component and its dominance over the viscoelastic component. The same behaviour is also expected to apply to fibrillated fibre surfaces.

- 4 The gel-likeness of the fibre surfaces can be assumed to play a notable role in transmitting forces already at low dry solids content. This has an impact on the consolidation of the fibre network, adhesion between fibres, transmittance of shrinkage forces and strength on the fibre bonds, and the fibre network structure.

## ACKNOWLEDGEMENTS

This research was part of the Academy of Finland-funded project ExtBioNet (tailored fibre-fibre interactions for boosted extensibility of bio-based fibre networks, decision No. 285627). The authors would like to thank Mr. Panu Lahtinen (Biomass processing, VTT, Espoo) for providing the fibrillated cellulose materials.

## REFERENCES

- [1] J. Strachan, "Further notes on the hydration of cellulose in papermaking," in *Proceedings of the Technical Section*, London, UK, 1932, p. 61.
- [2] J. D. Clark, "New thoughts on cellulose bonding," *TAPPI J.*, vol. 67, no. 12, pp. 82–83, 1984.
- [3] J. Clark, "Fibrillation, free water, and fiber bonding," *Tappi*, vol. 52, no. 2, p. 335, 1969.
- [4] H. Nanko and K. Ohsawa, "Mechanisms of fibre bond formation," in *Fundamentals of Papermaking, Transactions of the 9th Fundamental Research Symposium*, C. Baker and V. Punton, Eds. Cambridge, UK: Mechanical Engineering Publications Limited, London, 1989, pp. 783–832.
- [5] R. Pelton, "A model of the external surface of wood pulp fibers," *Nord. Pulp Pap. Res. J.*, vol. 11, no. 1, pp. 113–119, 1993.
- [6] H. Higgins and J. De Yong, "The beating process – primary effects and their influence on paper properties," in *Transactions of the 2nd Fundamental Research Symposium*, Oxford, UK, 1961, pp. 651–690.
- [7] H. Giertz, "Contribution to the theory of tensile strength," in *EUCEPA/European TAPPI Conference on Beating*, Venice, Italy, 1964, pp. 39–47.
- [8] T. Kang, "Role of external fibrillation in pulp and paper properties," Helsinki University of Technology, 2007.
- [9] F. W. Herrick, R. L. Casebier, J. Hamilton and K. Sandberg, "Microfibrillated cellulose morphology and accessibility," in *J. App. Polym. Sci. Symp. (Proc Cellul Conf, 9th, Part 2)*, 1982, pp. (37) 797-813.
- [10] L. Heux, E. Dinand and M. R. Vignon, "Structural aspects in ultrathin cellulose microfibrils followed by <sup>13</sup>C CP-MAS NMR," *Carbohydr. Polym.*, vol. 40, no. 2, pp. 115–124, 1999.

- [11] M. Andresen, L.-S. Johansson, B. S. Tanem and P. Stenius, "Properties and characterization of hydrophobized microfibrillated cellulose," *Cellulose*, vol. 13, no. 6, pp. 665–677, Sep. 2006.
- [12] H. Giertz, "Understanding the role of fines," in *International Symposium of Fundamental Concepts of Refining*, Appleton, WI, USA, 1980, pp. 324–333.
- [13] T. Saito and A. Isogai, "TEMPO-mediated oxidation of native cellulose. The effect of oxidation conditions on chemical and crystal structures of the waterinsoluble fractions," *Biomacromolecules*, vol. 5, no. 5, pp. 1983–1989, 2004.
- [14] E. Retulainen, K. Luukko, K. Fagerholm, J. Pere, J. Laine and H. Paulapuro, "Paper-making quality of fines from different pulps – the effect of size, shape and chemical composition," *Appita*, vol. 55, no. 6, pp. 457–467, 2002.
- [15] E. Retulainen, P. Moss and K. Nieminen, "Effect of fines on the properties of fibre networks," in *Trans. 10th Fund. Res. Symp*, Oxford, Pira International, Leatherhead, UK, 1993, pp. 727–769.
- [16] T. Taipale, M. Österberg, A. Nykänen, J. Ruokolainen and J. Laine, "Effect of microfibrillated cellulose and fines on the drainage of kraft pulp suspension and paper strength," *Cellulose*, vol. 17, no. 5, pp. 1005–1020, 2010.
- [17] M. L. Hassan, J. Bras, E. Mauret, S. M. Fadel, E. A. Hassan and N. A. ElWakil, "Palm rachis microfibrillated cellulose and oxidized-microfibrillated cellulose for improving paper sheets properties of unbeaten softwood and bagasse pulps," *Ind. Crops Prod.*, vol. 64, pp. 9–15, 2015.
- [18] A. Turbak, F. Snyder and K. Sandberg, "Microfibrillated cellulose, a new cellulose product: Properties, uses, and commercial potential," *J. Appl. Polym. Sci. Appl. Polym. Symp.*, vol. 37, pp. 815–827, 1983.
- [19] M. Pääkko et al., "Enzymatic hydrolysis combined with mechanical shearing and high-pressure homogenization for nanoscale cellulose fibrils and strong gels," *Biomacromolecules*, vol. 8, no. 6, pp. 1934–1941, 2007.
- [20] P. Lahtinen, S. Liukkonen, J. Pere, A. Sneck and H. Kangas, "A Comparative study of fibrillated fibers from different mechanical and chemical pulps," *BioResources*, vol. 9, no. 2, pp. 2115–2127, 2014.
- [21] S. Varanasi, R. He and W. Batchelor, "Estimation of cellulose nanofibre aspect ratio from measurements of fibre suspension gel point," *Cellulose*, vol. 20, no. 4, pp. 1885–1896, 2013.
- [22] R. Tanaka, T. Saito, H. Hondo and A. Isogai, "Influence of flexibility and dimensions of nanocelluloses on the flow properties of their aqueous dispersions," *Biomacromolecules*, vol. 16, no. 7, pp. 2127–2131, Jul. 2015.
- [23] M. Pääkkö et al., "Long and entangled native cellulose i nanofibers allow flexible aerogels and hierarchically porous templates for functionalities," *Soft Matter*, vol. 4, no. 12, pp. 2492–2499, 2008.
- [24] K. L. Spence, R. A. Venditti, O. J. Rojas, Y. Habibi and J. J. Pawlak, "A comparative study of energy consumption and physical properties of microfibrillated cellulose produced by different processing methods," *Cellulose*, vol. 18, no. 4, pp. 1097–1111, 2011.



- [25] A. E. Ketola et al., “Cellulose nanofibrils prepared by gentle drying methods reveal the limits of helium ion microscopy imaging,” *RSC Adv.*, vol. 9, no. 27, pp. 15668–15677, 2019.
- [26] H. Sehaqui, Q. Zhou, O. Ikkala and L. A. Berglund, “Strong and Tough Cellulose Nanopaper with High Specific Surface Area and Porosity,” *Biomacromolecules*, vol. 12, no. 10, pp. 3638–3644, Oct. 2011.
- [27] S. Arola, M. Ansari, A. Oksanen, E. Retulainen, S. G. Hatzikiriakos and H. Brumer, “The sol–gel transition of ultra-low solid content TEMPO-cellulose nanofibril/mixed-linkage  $\beta$ -glucan bionanocomposite gels,” *Soft Matter*, vol. 14, no. 46, pp. 9393–9401, Nov. 2018.
- [28] J. Goodwin and R. Hughes, *Rheology for Chemists: An Introduction*, 2nd ed. Cambridge, UK: Royal Society of Chemistry, 2008.
- [29] S. Fält, L. Wågberg and E.-L. Vesterlind, “Swelling of Model Films of Cellulose Having Different Charge Densities and Comparison to the Swelling Behavior of Corresponding Fibers,” *Langmuir*, vol. 19, pp. 7895–7903, 2003.
- [30] E. Kontturi, T. Tammelin and M. Österberg, “Cellulose-model films and the fundamental approach,” *Chem. Soc. Rev.*, vol. 35, pp. 1287–1304, 2006.
- [31] P. Myllytie, S. Holappa, J. Paltakari and J. Laine, “Effect of polymers on aggregation of cellulose fibrils and its implication on strength development in wet paper web,” *Nord. Pulp Pap. Res. J.*, vol. 24, no. 2, pp. 125–134, 2009.
- [32] T. Tammelin, T. Saarinen, M. Österberg and J. Laine, “Preparation of Langmuir/Blodgett-cellulose Surfaces by Using Horizontal Dipping Procedure. Application for Polyelectrolyte Adsorption Studies Performed with QCM-D,” *Cellulose*, vol. 13, no. 5, pp. 519–535, Oct. 2006.
- [33] S. Ahola, J. Salmi, L. S. Johansson, J. Laine and M. Österberg, “Model films from native cellulose nanofibrils. Preparation, swelling, and surface interactions,” *Biomacromolecules*, vol. 9, no. 4, pp. 1273–1282, 2008.
- [34] P. Myllytie, “Interactions of Polymers With Fibrillar Structure of Cellulose Fibres : a New Approach To Bonding and Strength in Paper,” Helsinki University of technology, 2009.
- [35] N. Chhabra, J. K. Spelt, C. M. Yip and M. T. Kortschot, “An investigation of pulp fibre surfaces by atomic force microscopy,” *J. Pulp Pap. Sci.*, vol. 31, no. 1, pp. 52–56, 2005.
- [36] F. Gu, W. Wang, Z. Cai, F. Xue, Y. Jin and J. Y. Zhu, “Water retention value for characterizing fibrillation degree of cellulosic fibers at micro and nanometer scales,” *Cellulose*, vol. 25, no. 5, pp. 2861–2871, 2018.
- [37] I. Duchesne and G. Daniel, “The ultrastructure of wood fibre surfaces as shown by a variety of microscopical methods – A review,” *Nord. Pulp Pap. Res. J.*, vol. 14, no. 2, pp. 129–139, 1999.
- [38] G. Chinga-Carrasco, Y. Yu and O. Diserud, “Quantitative electron microscopy of cellulose nanofibril structures from eucalyptus and pinus radiata kraft pulp fibers,” *Microsc. Microanal.*, vol. 17, no. 4, pp. 563–571, 2011.
- [39] J. Belle, S. Kleemann, J. Odermatt and A. Olbrich, “A new method showing the impact of pulp refining on fiber–fiber interactions in wet webs,” *Nord. Pulp Pap. Res. J.*, vol. 31, no. 2, pp. 205–212, 2016.

- [40] H. Kangas, P. Lahtinen, A. Sneek, A.-M. Saariaho, O. Laitinen and E. Hellén, “Characterization of fibrillated celluloses. A short review and evaluation of characteristics with a combination of methods,” *Nord. Pulp Pap. Res. J.*, vol. 29, no. 1, pp. 129–43, 2014.
- [41] K. Abe, S. Iwamoto and H. Yano, “Obtaining cellulose nanofibers with a uniform width of 15 nm from wood,” *Biomacromolecules*, vol. 8, no. 10, pp. 3276–3278, 2007.
- [42] S. Ahola, M. Österberg and J. Laine, “Cellulose nanofibrils – Adsorption with poly(amideamine) epichlorohydrin studied by QCM-D and application as a paper strength additive,” *Cellulose*, vol. 15, no. 2, pp. 303–314, 2008.
- [43] M. T. Postek, A. E. Vladar, J. Kramar, L. A. Stern, J. Notte and S. McVey, “Helium ion microscopy: A new technique for semiconductor metrology and nanotechnology,” *AIP Conf. Proc.*, vol. 931, no. 2007, pp. 161–167, 2007.
- [44] M. T. Postek et al., “Development of the metrology and imaging of cellulose nanocrystals,” *Meas. Sci. Technol.*, vol. 22, no. 2, p. 024005, Feb. 2011.
- [45] B. W. Ward, J. A. Notte and N. P. Economou, “Helium ion microscope: A new tool for nanoscale microscopy and metrology,” *J. Vac. Sci. Technol. B Microelectron. Nanom. Struct.*, vol. 24, no. 6, p. 2871, Nov. 2006.
- [46] K. K. Kesari et al., “Chemical characterization and ultrastructure study of pulp fibers,” *Mater. Today Chem.*, vol. 17, 2020.
- [47] Z. Li, J. Liu, K. Jiang and T. Thundat, “Carbonized nanocellulose sustainably boosts the performance of activated carbon in ionic liquid supercapacitors,” *Nano Energy*, vol. 25, pp. 161–169, Jul. 2016.
- [48] J. Virtanen, M. Janka and S. Tuukkanen, “Fabrication and characterization of nanocellulose aerogel structures,” in *EMBEC & NBC 2017, IFMBE Proceedings 65*, 2018, pp. 1029–1032.
- [49] K. Torvinen et al., “Nanoporous kaolin – cellulose nano fibril composites for printed electronics,” *Flex. Print. Electron.*, vol. 2, no. 024004, 2017.
- [50] J. T. Korhonen, P. Hiekkataipale, J. Malm, M. Karppinen, O. Ikkala and R. H. A. Ras, “Inorganic Hollow Nanotube Aerogels by Atomic Layer Deposition onto Native Nanocellulose Templates,” *ACS Nano*, vol. 5, no. 3, pp. 1967–1974, Mar. 2011.
- [51] A. Strand et al., “The effect of chemical additives on the strength, stiffness and elongation potential of paper,” *Nord. Pulp Pap. Res. J.*, vol. 32, no. 3, pp. 324–335, 2017.
- [52] J. Vartiainen and T. Malm, “Surface hydrophobization of CNF films by roll-to-roll HMDSO plasma deposition,” *J. Coatings Technol. Res.*, vol. 13, no. 6, pp. 1145–1149, 2016.
- [53] S. H. Osong, S. Norgren, P. Engstrand, M. Lundberg, M. Reza and V. Tapani, “Qualitative evaluation of microfibrillated cellulose using the crill method and some aspects of microscopy,” *Cellulose*, vol. 23, no. 6, pp. 3611–3624, 2016.
- [54] S. H. Osong, S. Norgren, P. Engstrand, M. Lundberg and P. Hansen, “Crill : A novel technique to characterize nano-ligno-cellulose,” vol. 29, no. 2, 2014.
- [55] N. Lavoine and L. Bergström, “Nanocellulose-based foams and aerogels: processing, properties, and applications,” *J. Mater. Chem. A*, vol. 5, no. 31, pp. 16105–16117, Aug. 2017.
- [56] J. T. Korhonen, M. Kettunen, R. H. A. Ras and O. Ikkala, “Hydrophobic nanocellulose aerogels as floating, sustainable, reusable, and recyclable oil absorbents,” *ACS Appl. Mater. Interfaces*, vol. 3, no. 6, pp. 1813–1816, 2011.

- [57] H. Jin, Y. Nishiyama, M. Wada and S. Kuga, “Nanofibrillar cellulose aerogels,” *Colloids Surfaces A Physicochem. Eng. Asp.*, vol. 240, no. 1–3, pp. 63–67, Jun. 2004.
- [58] M. Kettunen et al., “Photoswitchable Superabsorbency Based on Nanocellulose Aerogels,” *Adv. Funct. Mater.*, vol. 21, no. 3, pp. 510–517, Feb. 2011.
- [59] T. Okamoto and G. Meshitsuka, “Determination of the Surface Layer of Kraft Pulp fibers by field emission Scanning electron microscope (FE-SEM),” 2003.
- [60] M. Leppänen, L.-R. Sundberg, E. Laanto, G. M. de Freitas Almeida, P. Papponen and I. J. Maasilta, “Imaging Bacterial Colonies and PhageBacterium Interaction at Sub-Nanometer Resolution Using Helium-Ion Microscopy,” *Adv. Biosyst.*, vol. 1700070, pp. 1–8, 2017.
- [61] B. G. Ershov, “Radiation-chemical degradation of cellulose and other polysaccharides,” *Russ. Chem. Rev.*, vol. 315, no. 4, pp. 315–334, 1998.
- [62] M. Iotti, Ø. W. Gregersen, S. Moe and M. Lenes, “Rheological Studies of Microfibrillar Cellulose Water Dispersions,” *J. Polym. Environ.*, vol. 19, no. 1, pp. 137–145, 2011.
- [63] O. Nechyporchuk, M. N. Belgacem and F. Pignon, “Rheological properties of micro-/nanofibrillated cellulose suspensions: Wall-slip and shear banding phenomena,” *Carbohydr. Polym.*, vol. 112, pp. 432–439, 2014.
- [64] A. I. Koponen, “The effect of consistency on the shear rheology of aqueous suspensions of cellulose micro- and nanofibrils: a review,” *Cellulose*, vol. 27, no. 4, pp. 1879–1897, Mar. 2020.
- [65] E. Retulainen, J. Parkkonen and A. Miettinen, “X-ray nanotomography of fibre bonds,” in *Progress in Paper Physics Seminar*, 2016, pp. 162–168.
- [66] T. Sormunen, A. Ketola, A. Miettinen, J. Parkkonen and E. Retulainen, “XRray Nanotomography of Individual Pulp Fibre Bonds Reveals the Effect of Wall Thickness on Contact Area,” *Sci. Rep.*, vol. 9, no. 1, p. 4258, 2019.
- [67] A. E. Ketola et al., “Effect of Micro- and Nanofibrillated Cellulose on the Drying Shrinkage, Extensibility, and Strength of Fibre Networks,” *BioResources*, vol. 13, no. 3, pp. 5319–5342, 2018.
- [68] Q. Tarrés, M. Delgado-Aguilar, M. A. Pèlach, I. González, S. Boufi and P. Mutjé, “Remarkable increase of paper strength by combining enzymatic cellulose nanofibers in bulk and TEMPO-oxidized nanofibers as coating,” *Cellulose*, vol. 23, no. 6, pp. 3939–3950, 2016.
- [69] Ø. Eriksen, “The use of microfibrillated cellulose produced from kraft pulp as strength enhancer in TMP paper,” *Nord. Pulp Pap. Res. J.*, vol. 23, no. 03, pp. 299–304, 2008.
- [70] D. Page and P. Tydeman, “Physical processes occurring during the drying phase,” in *Consolidation of the Paper Web*, Trans. 3rd., F. Bolam, Ed. Manchester: FRC, 1965, pp. 371–392.
- [71] A. K. Vainio and H. Paulapuro, “Interfiber bonding and fiber segment activation in paper,” *BioResources*, vol. 2, no. 3, pp. 442–458, 2007.
- [72] A. Vainio and H. Paulapuro, “Observations on interfibre bonding and fibre segment activation based on the strength properties of laboratory sheets,” *Nord. Pulp Pap. Res. J.*, vol. 20, no. 3, pp. 340–344, 2005.

*A. E. Ketola, M. Leppänen, T. Turpeinen et al.*

- [73] J. Laine, T. Lindstrom, C. Bremberg and G. Glad-Nordmark, "Studies on topochemical modification of cellulosic fibres," *Nord. Pulp Pap. Res. J.*, vol. 18, no. 3, pp. 325–332, 2007.
- [74] H. Liimatainen, S. Haavisto, A. Haapala and J. Niinimäki, "Influence of adsorbed and dissolved carboxymethyl cellulose on fibre suspension dispersing, dewaterability, and fines retention," *BioResources*, vol. 4, no. 1, pp. 321–340, 2009.
- [75] H. Yan, T. Lindström and M. Christiernin, "Some ways to decrease fibre suspension flocculation and improve sheet formation," *Nord. Pulp Pap. Res. J.*, vol. 21, no. 1, pp. 36–43, 2006.